Article:
Shields, GA, Mills, BJW orcid.org/0000-0002-9141-0931, Zhu, M et al. (3 more authors) (2019) Unique Neoproterozoic carbon isotope excursions sustained by coupled evaporite dissolution and pyrite burial. Nature Geoscience, 12 (10). pp. 823-827. ISSN 1752-0894

https://doi.org/10.1038/s41561-019-0434-3

Unique Neoproterozoic carbon isotope excursions sustained by coupled evaporite dissolution and pyrite burial

Graham A. Shields[1], Benjamin J.W. Mills[2], Maoyan Zhu [3,4], Timothy D. Raub[5] Stuart Daines[6] & Timothy M. Lenton[6]

[1]Department of Earth Sciences, University College London, Gower Place, London, WC1E 6BT, UK

[2]School of Earth and Environment, University of Leeds, Leeds, LS2 9JT, UK

[3]State Key Laboratory of Palaeobiology and Stratigraphy & Center for Excellence in Life and Paleoenvironment, Nanjing Institute of Geology and Palaeontology, Chinese Academy of Sciences, Nanjing, 210008, China

[4]College of Earth Sciences, University of Chinese Academy of Sciences, Beijing, 100049, China

[5]School of Earth and Environmental Sciences, University of St. Andrews, KY16 9AL, UK

[6] Global Systems Institute, University of Exeter, Exeter, EX4 4QE, UK

Correspondence and requests for materials should be addressed to G.S. (g.shields@ucl.ac.uk), B.M (b.mills@leeds.ac.uk) or M.Z. (myzhu@nigpas.ac.cn)

The Neoproterozoic Era witnessed a succession of biological innovations that culminated in a wide range of animal body plans and behaviours during the Ediacaran-Cambrian radiations. Intriguingly, this interval is also marked by perturbations to the global carbon cycle, as evidenced by extreme fluctuations in climate and carbon isotopes. The Neoproterozoic isotope record has defied parsimonious explanation because sustained ^{12}C-enrichment (low δ^{13}C) in seawater seems to imply that substantially more oxygen was consumed by organic carbon oxidation than could possibly have been available. Here we propose a solution to this problem, in which carbon and oxygen cycles can maintain dynamic equilibrium during negative δ^{13}C excursions when surplus oxidant is generated through bacterial reduction of sulfate that originates from evaporite weathering. Coupling of evaporite dissolution with pyrite burial drives a positive feedback loop whereby net oxidation of marine organic carbon can sustain greenhouse forcing of chemical weathering, nutrient input and ocean margin euxinia. Our proposed model is particularly applicable to the late Ediacaran 'Shuram' isotope excursion that directly preceded the emergence of energetic metazoan metabolisms during the Ediacaran-Cambrian transition. Non-steady state sulfate dynamics are likely to have contributed to climate change, episodic ocean oxygenation and opportunistic radiations of aerobic life forms during the Neoproterozoic Era.

The Neoproterozoic Era (1000 – c.540 Ma) marks a turning point in Earth history when groups of morphologically complex multicellular eukaryotes, including algae and animals, attained ecological dominance, irrevocably changing Earth System dynamics[1]. These biological radiations took place amid fluctuating climate, including two prolonged episodes of global glaciation during the Cryogenian Period (c.715 – c.660 and c.650 – c.635 Ma) and short-lived, regional ice ages during the Ediacaran Period (e.g. c.580 Ma), interspersed with warmer

intervals. The world's oceans also became episodically more oxygenated during the Neoproterozoic with the extent of oxygenated seafloor reaching near-modern levels at times during the early Cambrian[2]. Both climate and oxygenation are regulated by Earth's long-term carbon cycle, and so perhaps unsurprisingly this interval is characterised by extreme carbon isotope instability[3] (Fig. 1). Since their discovery over 30 years ago[4–7], the uniquely high amplitudes of Neoproterozoic $\delta^{13}C$ excursions have defied conventional interpretation[3,8–10]. Here we relate the largest of these anomalies to the transfer of oxidant from the evaporite rock reservoir to the surface environment via the coupling of sulfate weathering and pyrite burial. Such pulses of evaporite weathering are predicted to have occurred during the Ediacaran Period (see detailed account in SI 4), in particular, as Rodinia's passive margins underwent tectonic uplift during the amalgamation of Gondwanaland[11].

Conventional carbon isotope mass balance is based on the principle that the isotopic composition of carbon input via outgassing and weathering, and that of sedimentary carbon outputs are equal on time scales of $>10^5$ years. This $\delta^{13}C$ value is considered to be unchanging at -5‰, which is taken to be the average composition of crustal carbon. Because organic matter is depleted in ^{13}C, and carbonate rocks precipitate in isotopic equilibrium with ambient dissolved inorganic carbon (DIC), the mean $\delta^{13}C$ value of carbonate rocks and fossils can be used to determine the proportion that sedimentary organic matter makes up of the total sedimentary carbon sink. This proportion is generally referred to as f_{org}, which has varied over Earth history between 0.1 and 0.3[12]. During the Neoproterozoic Era, globally correlative marine carbonate rocks from at least three intervals (~720 Ma Garvellach[13], ~650 Ma Trezona[14,15], ~560 Ma Shuram[5,16]/Wonoka[7]/DOUNCE[17] anomalies) are characterised by $\delta^{13}C$ values below -5‰ (Fig. 1), which can, using a conventional mass balance approach, only be explained by negative rates of organic burial. This is particularly true of the late Ediacaran Shuram excursion, during which $\delta^{13}C$ remained below -8‰ for at least ~10 Myr[18,19]. In order

to address this quandary, it was proposed that the pool of dissolved organic matter (DOM) in the Proterozoic ocean was much larger than today, and that negative excursions represent non-steady-state remineralisation of that pool[3]. However, later numerical treatments of this model[20,21] pointed out that the Earth system cannot remain out of oxygen (and carbon) balance for such a long period of time. In other words, there is insufficient oxidant even in the modern atmosphere and oceans to remineralise enough organic matter to drive a -8‰ $\delta^{13}C$ excursion for several million years. As a result, many authors have interpreted extreme negative anomalies as diagenetic alteration[22], authigenic cements[10] or as regional phenomena[23]. However, such arguments appeal to an inexplicable sampling bias, whereby globally correlative isotopic signatures are presumed to be unrepresentative of the global carbonate sink.

Here we take a different approach to the problem of negative $\delta^{13}C$ excursions by viewing them in terms of a linked carbon-sulfur-oxygen system, whereby changes in oxidant dynamics caused an excess of organic carbon oxidation over burial, resulting in a smaller DOM reservoir. For steady state to be maintained throughout a negative $\delta^{13}C$ excursion, shrinkage of the DOM pool would need to match surplus oxidant production for the duration of the anomaly. If we consider plausible $\delta^{13}C$ values of -10‰[17] and -35‰ for deposited carbonates and kerogen (globally averaged carbon sinks), respectively, and -30‰[24] and -5‰ for the DOM reservoir and crustal carbon (globally averaged carbon sources), respectively, then organic carbon oxidation would need to increase over the background rate by approximately a factor of three (Methods 1). This oxidant imbalance then requires three times as much oxygen as could have been supplied by organic burial alone. Therefore, it can only plausibly be sustained via the other major net source of oxygen to the Earth system: pyrite burial.

Although bacterial sulfate reduction coupled with pyrite burial releases on a mole-for-mole basis almost twice as much oxygen as organic burial[25], it is generally assumed that the oxygen released by pyrite burial is approximately matched by the oxygen consumed during pyrite

98 weathering. However, most riverine sulfate derives from the weathering of evaporites[26], rates
99 of which due to the sporadic and regional nature of evaporite deposits, will vary considerably
100 over time[27]. During parts of the Proterozoic, when oceans were both iron-rich and anoxic[28],
101 and so prone to sulfate reducing conditions (euxinia) at productive margins, one might
102 realistically suppose that the amount of oxidising power transferred from rock sulfate to the
103 surface environment would also have varied considerably, particularly during times when no
104 basin-scale evaporite deposits were forming.

105 By writing a simple steady state mass-balance for the surface carbon cycle (Methods 1) we can
106 map the broad relationship between the evaporite sulfate input rate, net DOM oxidation and
107 $\delta^{13}C$ composition of the ocean-atmosphere system (Fig. 2). These calculations show that an
108 evaporite weathering flux of around 1.1×10^{13} mol S yr^{-1} (around 10 times the modern flux,
109 as proposed for the dissolution event during the early Cenozoic[27]) could sustain a carbon
110 isotope excursion of between -10‰ and -15‰, depending on the proportion of the riverine
111 sulfate flux that is eventually buried as pyrite. Thus, the amount of oxidant required to achieve
112 a deep negative carbon isotope excursion through net organic carbon oxidation may reasonably
113 result from basin-scale evaporite dissolution.

114 Although plausible, we acknowledge that the above steady-state approximation is highly
115 idealised and does not capture the true dynamics of the expected events, which include both
116 positive and negative feedbacks (Fig. 3). For a negative $\delta^{13}C$ excursion to be generated, oxidant
117 input needs to be coupled to shrinkage of a marine DOM reservoir, rather than accumulating
118 as an atmospheric oxygen increase. The rate of DOM oxidation is controlled by the deep ocean
119 redox state, which itself is largely controlled by the abundance of atmospheric oxygen.
120 Therefore, the process of DOM oxidation must be self-limiting and it should not be possible to
121 deplete the surface oxygen reservoir beyond the level that causes the deep ocean to become
122 entirely anoxic. Net oxidation of organic carbon should cause a substantial rise in atmospheric

CO_2 concentration and hence additional climate feedbacks. Rising CO_2 and temperature would support enhanced continental weathering, with the potential to drive further evaporite dissolution and therefore sustain oxidant delivery.

The network of long-term biogeochemical feedbacks between the sulfur, carbon and oxygen cycles is adequately represented by the COPSE biogeochemical box model[29], and in order to explore how changes in the evaporite sulfate weathering flux might affect the oxidant balance in a Proterozoic marine environment, we modify COPSE to include a dynamic reservoir of deep-ocean DOM (modelled as DOC) and an extra input flux of sulfate from weathering (Methods 2 and SI). The model is first set up for an 'Ediacaran like' steady state (pO_2 = 0.05 PAL, pCO_2 = 13 PAL, SO_4 = 0.1 of present ocean level and a mostly anoxic deep ocean). This is achieved by fixing background tectonic parameters (uplift, degassing) at assumed values for 600 Ma, while lowering the phosphorus input rate by 50%[30].

We then perturb the system by adding a weathering pulse of sulfate from evaporite dissolution, and a smaller pulse of sulfate from pyrite oxidation, assuming that pyrite-bearing sediments would also be exposed during uplift. These pulses follow simple stepwise increases and decreases[27], but also include a dependence on climate through runoff as summarized in figure 3 (see methods for details). Figure 4a shows the overall amount of S delivery from evaporite dissolution ($\sim 50 - \sim 100 \times 10^{18}$ mol), which is chosen to be similar to that proposed for basin-scale evaporite dissolution in the Cenozoic (~1.1×10^{13} mol S yr^{-1} for ~5 Myrs)[27], although we use a longer timeframe to compare to the long duration of the Shuram excursion. The control model run with no DOC reservoir is shown in grey in figure 4. As shown previously[27], this level of sulfate input raises ocean sulfate concentration considerably. Increased burial of pyrite leads to a substantial increase in pO_2 and less prevalence of anoxia (shown as fraction of anoxic seafloor). Oxidative weathering of fossil organic carbon increases as O_2 rises, causing a small reduction in $\delta^{13}C$ and increase in pCO_2. Seawater $\delta^{34}S$ decreases

148 during the evaporite dissolution event as the combined $\delta^{34}S$ value of inputted evaporite and
149 pyrite sulfur is lower than the initial seawater value (we set $\delta^{34}S_{pyr}$ = 0‰ and $\delta^{34}S_{evap}$ = 15‰
150 for the weathered material cf.[31]). The increase in pyrite burial buffers against this change by
151 driving $\delta^{34}S$ to more positive values (manifest as a 'hump' in the model $\delta^{34}S$ curve), but is
152 insufficient to reverse the overall trend.

153 We view net oxidation of deep ocean DOC as a feedback process driven by other model
154 variables, and model it accordingly. Model runs include a DOC reservoir of size 20 times (light
155 blue) and 30 times (dark blue) the modern DIC reservoir, respectively. The reservoir is assumed
156 to have a carbon isotopic composition of -30‰ and is allowed to be oxidized when the degree
157 of anoxia (ANOX) is reduced below a threshold value (see Methods 2). In both runs, oxidation
158 of DOC begins as the deep ocean becomes more widely oxygenated, however, as DOC
159 oxidation is an oxygen sink, ANOX remains at the threshold value until the DOC reservoir
160 nears depletion. In this period, the model is in a quasi-steady state wherein the transition to an
161 oxygenated deep ocean is prevented by the net oxidation of DOC. During this state, ocean $\delta^{13}C$
162 is around -9‰, close to the value suggested by the simple calculations shown in Figure 2 for
163 this level of sulfate input. Persistent anoxia, nutrient delivery, and the related increase in pyrite
164 burial rates drive $\delta^{34}S$ values higher than the control run, but the model still produces a negative
165 excursion in $\delta^{34}S$, consistent with available observations[16,32]. On depletion of the DOC
166 reservoir, the deep ocean can be oxygenated, and the model gradually returns to follow the
167 control experiment.

168 The duration of the carbon isotope anomaly in our COPSE model reconstruction depends on
169 the size of the DOM pool and on being able to maintain high rates of pyrite burial, but crucially
170 does not depend on (or deplete) the atmospheric O_2 pool, which is predicted to increase during
171 the course of the excursion. A high rate of pyrite burial would be maintained in part due to the
172 effect of organic remineralisation on raising pCO_2 and global temperatures, which produces a

positive feedback loop (Fig. 3), whereby high chemical weathering rates and nutrient input can sustain euxinic ocean margins until either the DOM pool or the evaporite weathering flux decreases below a certain threshold value. Our treatment of these aspects is necessarily simple: we assume in the model run shown that 80% of the inputted sulfate is buried as pyrite by a near-shore biota that is sensitive to river inputs[33]. We also assume that gypsum, pyrite and organic carbon weathering fluxes are related to the model global rate of runoff (in addition to following a prescribed stepwise increase and decrease for pyrite and gypsum). We show further model runs in the SI in which the climate-weathering effect is not considered, and in which only evaporite inputs are considered, without any weathering of pyrite. We also show runs where differing amounts of P release from DOM oxidation fuels additional primary productivity. Sustained, highly-negative $\delta^{13}C$ excursions remain possible in all of these cases, but a closely corresponding negative $\delta^{34}S$ excursion can only be achieved when a smaller pulse of pyrite weathering accompanies the evaporite weathering pulse. While pyrite weathering is important in setting seawater $\delta^{34}S$ values, pyrite weathering and deposition form an O_2-neutral cycle over long timescales so other model processes are relatively unaffected.

This evaporite dissolution / DOM oxidation scenario appears to be the most parsimonious solution to the Shuram C-isotope conundrum in that it predicts the extent of oxic seafloor to increase towards the end of the excursion, while maintaining high sulfate concentrations, which is in line with geochemical studies[34,35]. Furthermore, the Shuram anomaly coincided with orogenic uplift relating to the formation of Gondwanaland[36], and in particular the tectonic inversion of all major basin-scale evaporite sulfate deposits of Tonian age (see SI 4). Although our model fits best the late Ediacaran Shuram anomaly, coupled evaporite dissolution and pyrite burial may have also played a role in other extreme negative carbon isotope excursions of the Neoproterozoic, which all occurred after one of the largest evaporite depositional events in Earth history between c.830 Ma and c.770 Ma[37]. The succeeding interval of major carbon

cycle disruption from c.770 Ma until c.550 Ma was a time of little or no basin-scale evaporite deposition, suggesting that, as in the Cenozoic[5], the sulfate weathering-deposition cycle was not in steady-state. However, unlike the Cenozoic, the low atmospheric oxygen and anoxic deep ocean of the Neoproterozoic allowed evaporite-derived oxidizing power to be effectively transmitted into a negative $\delta^{13}C$ signal.

The existence of a series of negative carbon isotope excursions during much of the Neoproterozoic Era indicates that the DOM pool underwent dynamic size changes throughout this time, and served as a buffer against oxygenation and climate change, but only when the pool was sufficiently large. Exhaustion of the DOM pool may have occurred during the Shuram anomaly, suggesting that the expansion of aerobic Ediacaran fauna at that time was an opportunistic radiation in response to a transient oxidant surplus. But it is possible that a greatly-reduced DOM pool may have continued to wax and wane until well into the Cambrian Period, during which time geochemical evidence suggests that redox conditions on the seafloor reached modern proportions for the first time[2].

Acknowledgements

This work was supported by the NERC-NSFC programme 'Biosphere Evolution, Transitions and Resilience' through grant NE/P013643/1 to G.A.S. and M.Z. and NE/P013651/1 to T.M.L., by grant NE/R010129/1 to G.A.S. and B.J.W.M., a University of Leeds Academic Fellowship to B.J.W.M., and by the National Natural Science Foundation of China (41661134048) and Strategic Priority Research Program (B) of the Chinese Academy of Sciences (XDB18000000) to M.Z.

Author contributions

G.A.S. and B.J.W.M. conceived the project. B.J.W.M. created the model, which was revised from previous versions created by T.M.L., B.J.W.M. and S.D. All authors contributed to data interpretation and the writing of the manuscript.

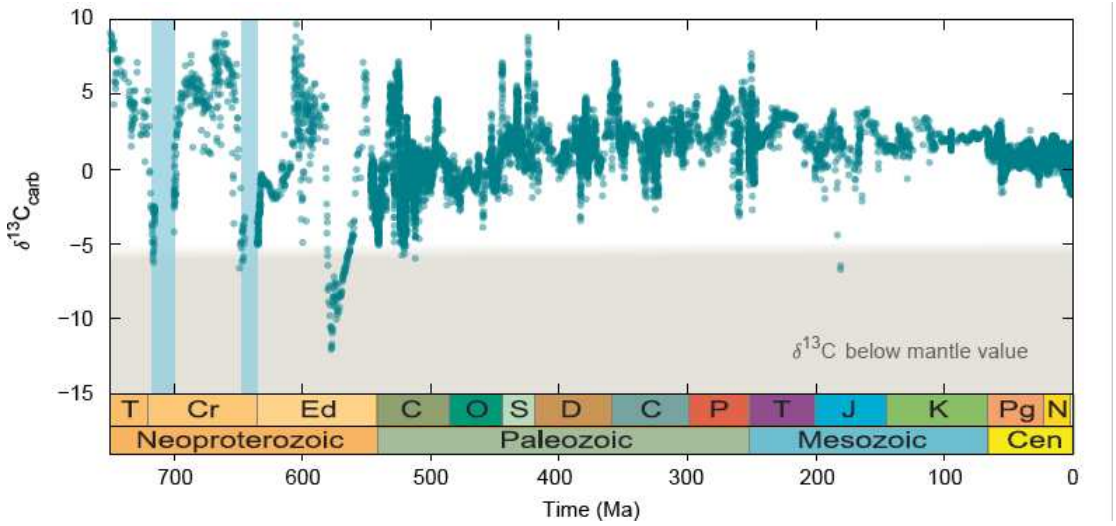

226

227 **Figure 1. Carbonate carbon isotope record (reproduced from [38]).** Grey area indicates values
228 below the average continental crust and mantle value of between -5‰ *and* -6‰ with three
229 major excursions at ~720 (Garvellach anomaly[13]), ~650 (Trezona anomaly[14]) and ~560 Ma
230 (Shuram anomaly[5,16]). Smaller post-glacial excursions occur after Cryogenian (Sturtian and
231 Marinoan) low latitude glacial events (blue bars). Black dashed line indicates progressive
232 deep ocean oxygenation between ~580 and ~520 Ma[39–41] . Note that excursions to below the
233 mantle value occur before and during deep-ocean oxygenation and climate events.

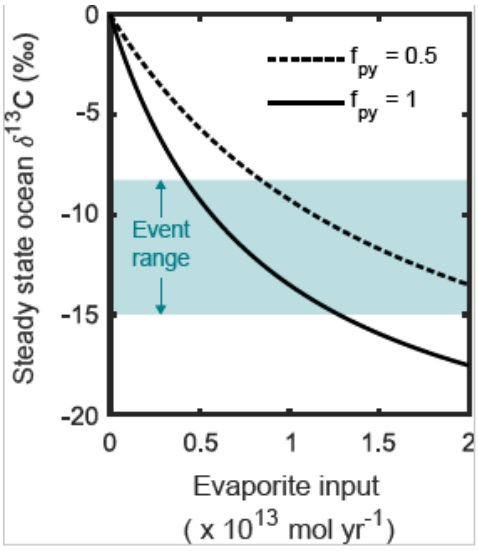

234

235 **Figure 2. Negative carbon isotope excursion driven by net oxidation of a dissolved organic**
236 **carbon reservoir via coupled evaporite weathering and pyrite burial.** The magnitude of the

237 $\delta^{13}C$ anomaly depends on the O_2 production rate from pyrite burial, which results from the
238 evaporite weathering flux and the fraction of this flux that is buried as pyrite.

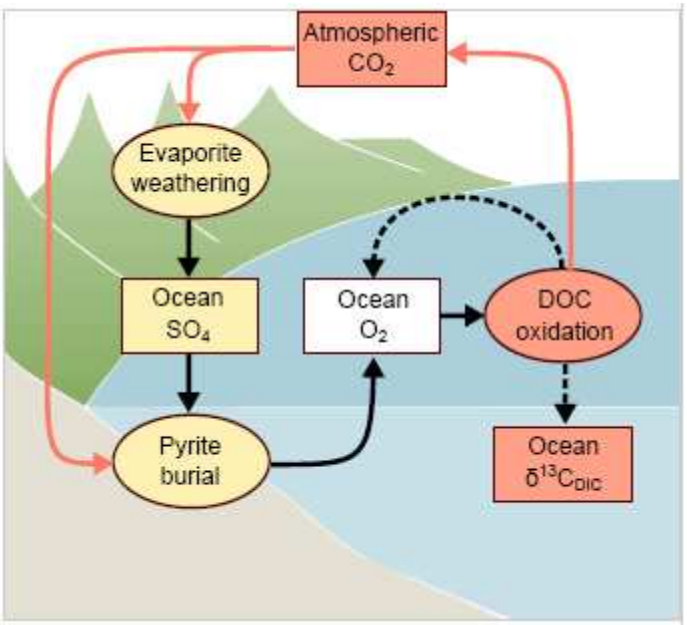

239

240 **Figure 3. Feedback diagram illustrating the effects of evaporite weathering on ocean**
241 ***oxygenation and* δ^{13}C.** Boxes show quantities, ovals show processes, whilst yellow indicates
242 sulfur cycle and red indicates carbon cycle. An evaporite dissolution event results in a large
243 flux of sulfate to the ocean, permitting high rates of pyrite burial, which increases
244 atmospheric and ocean O_2. As the deep ocean becomes oxygenated, depletion of the dissolved
245 organic carbon (DOC) reservoir represents a negative feedback on ocean oxygenation and
246 drives *ocean* $\delta^{13}C$ to negative values. Red arrows show potential for positive feedback: DOC
247 oxidation increases atmospheric CO_2, leading to higher surface temperature and greater
248 rates of precipitation and runoff, which fuels further evaporite dissolution and nutrient
249 delivery. Solid arrows show positive effects and dashed arrows show negative effects.

250

251

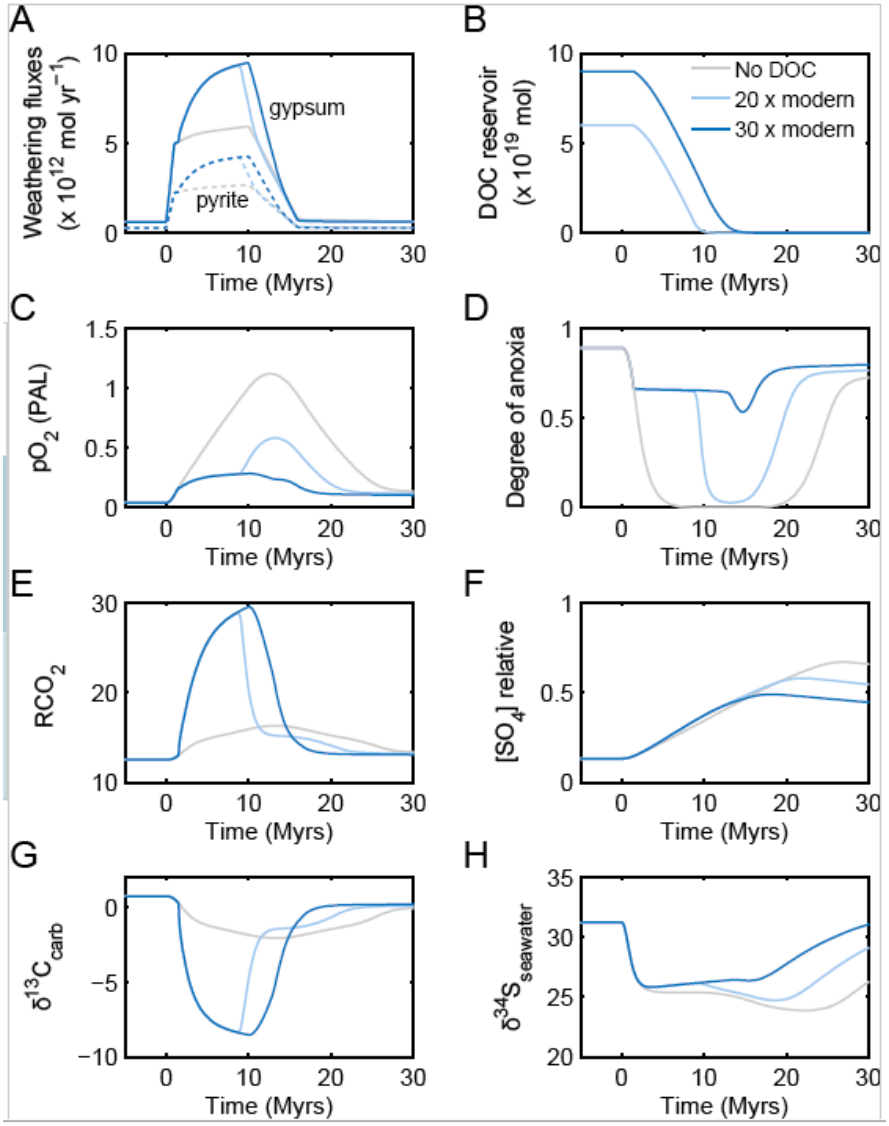

Figure 4. COPSE Model forced with sulfate input and including differently sized DOC reservoirs. A. Input rates of sulfate from gypsum and pyrite weathering. B. Size of DOC reservoir in moles of carbon. C. A. Relative atmospheric oxygen concentration. D. Degree of ocean anoxia. E. Relative atmospheric carbon dioxide concentration. F. Relative ocean sulfate *concentration. G. Calculated* δ^{13}C of new carbonate. H. Calculated *seawater* δ^{34}S.

Methods

1. Steady state mass balance calculations

In order to estimate the surplus oxygen flux needed to sustain the late Ediacaran Shuram anomaly, we apply standard isotope mass balance, and assume $\delta^{13}C$ values of -10‰[17] and -35‰ for deposited carbonates ($\delta^{13}C_{carb}$) and kerogen ($\delta^{13}C_{org}$), respectively, and -30‰[24] and -5‰ for the integrated carbon sources ($\delta^{13}C_{input}$) of DOM oxidation and crustal carbon, respectively. Following standard C-isotope mass balance, $\delta^{13}C_{carb} = (\Delta^{13}C_{carb\text{-}org}) \cdot f_{org} + \delta^{13}C_{input}$ at steady state, and so during the excursion when $f_{org} = 0.1$[12], then $\delta^{13}C_{input} = -12.5‰$. The proportion that DOM oxidation contributed to the global carbon cycle, i.e. f_{DOM}, = 0.3, whereby $\delta^{13}C_{excursion\ input} = -12.5‰ = \delta^{13}C_{pre\text{-}excursion\ input}(1\text{-}f_{DOM}) + \delta^{13}C_{DOM}.f_{DOM}$. A conservative estimate for the requisite surplus oxygen flux (f_{DOM}) would therefore be about three times greater than that supplied by organic burial (f_{org}) alone, thus requiring a contribution from other sources, most likely pyrite burial.

In order to explore the potential for evaporite dissolution to drive surface system oxygenation and negative carbon isotope excursions, we first solve a simple isotope mass balance calculation for the $\delta^{13}C$ composition of the total combined atmosphere and ocean carbon pool (A). Variations in A over time follow the formulation:

$$\frac{dA}{dt} = F_{oxidw} + F_{ocdeg} + F_{carbw} + F_{ccdeg} - F_{ocb} - F_{mccb} - F_{sfw} + F_{DOCox} \quad (1)$$

Where F_{oxidw} is oxidative weathering, F_{ocdeg} is organic carbon metamorphism and degassing, F_{carbw} is carbonate weathering, F_{ccdeg} is carbonate degassing, F_{ocb} is organic carbon burial, F_{mccb} is marine carbonate burial and F_{sfw} is seafloor weathering (following[29,21]). We add F_{DOCox} to represent the oxidation of a deep ocean reservoir of dissolved organic carbon. As a general approximation to the expected Ediacaran carbon cycle we take $F_{oxidw} = 2.5 \times 10^{12}$ mol yr^{-1}, $F_{ocdeg} = 0.5 \times 10^{12}$ mol yr^{-1}, $F_{carbw} = 8 \times 10^{12}$ mol

285 yr^{-1}, $F_{ccdeg} = 6 \times 10^{12}$ mol yr^{-1}, $F_{ocb} = 3 \times 10^{12}$ mol yr^{-1}, $F_{mccb} = 12 \times 10^{12}$ mol yr^{-1}, and
286 $F_{sfw} = 2 \times 10^{12}$ mol yr^{-1}. Here $\frac{dA}{dt} = 0$, thus the carbon cycle is in steady state, and the
287 fraction of carbon buried in organic form (f_{org}) is 0.2.

288 We assume that the sulfur cycle begins at steady state, and allow an addition of sulfate
289 from evaporite dissolution, F_{evap} (in moles S). To maintain long-term steady state this
290 evaporite must leave the system in oxidised (e.g. gypsum) or reduced (e.g. pyrite) forms. We
291 denote f_{py} as the fraction of the evaporite input that exits the system as pyrite and experiment
292 with values of 0.5 and 1. Assuming that DOC oxidation is driven solely by excess oxygen
293 produced by burial of pyrite, we set the flux of DOC oxidation as $F_{DOCox} = 2 \times f_{py} F_{evap}$. To
294 maintain long term steady state in the carbon cycle, the flux of additional CO_2 from DOC
295 oxidation must be balanced by burial of carbonates and organic carbon. We assume this
296 occurs at the initial ratio of 4:1 in favour of carbonates (e.g. $f_{org} = 0.2$). Thus the equation
297 for long term carbon isotopic mass balance is:

298 $$F_{oxidw}\delta_G + F_{ocdeg}\delta_G + F_{carbw}\delta_C + F_{ccdeg}\delta_C - F_{ocb}(\delta_A - \Delta B) - F_{mccb}\delta_A - F_{sfw}\delta_A +$$
299 $$F_{DOCox}\delta_{DOC} - 0.2F_{DOCox}(\delta_A - \Delta B) - 0.8F_{DOCox}\delta_A = 0 \qquad (2)$$

300 where δ_A is the isotopic composition of atmosphere and ocean carbon, δ_C is the compositions
301 of buried carbonates, δ_G is the composition of buried organic carbon and δ_{DOC} is the
302 composition of the oceanic DOC reservoir. We take $\delta_C = 0‰$, $\delta_G = -25‰$, $\Delta B = 25‰$,
303 $\delta_{DOC} = -30‰$, and solve for δ_A under varying values for F_{evap}. Results are shown in figure
304 2.

305

306 **2. COPSE model reconstructions**

We run the COPSE model[21] to steady state under assumed Ediacaran forcings, add a deep ocean reservoir of dissolved organic carbon that responds to the degree of ocean anoxia, then impose an evaporite dissolution and pyrite burial event.

Ediacaran steady state

The 'Ediacaran' steady state is achieved by fixing all model parameters at the assumed values for 600 Ma. In all but two cases, these values are assumed to be the same as at the beginning of the Phanerozoic, but we lower the rate of phosphorus input by 50% to reduce atmospheric oxygen (e.g. as in Daines et al. 2017[22]) and use a static gypsum burial rate of 50% of the present day to reduce ocean sulfate. The steady state has pO_2 = ~0.05 PAL, pCO_2 = ~13 PAL, SO_4 = ~0.1 of present ocean level and a mostly anoxic deep ocean (ANOX ≈ 0.9).

Dissolved organic carbon reservoir

The size of the model DOC reservoir is set at the beginning of the model run. The reservoir has a single output flux via DOC oxidation, which depends on the degree of ocean anoxia (ANOX):

$$\frac{dDOC}{dt} = \begin{cases} 0\,, & DOC < 1 \times 10^{12}\ mol \\ -\frac{k}{1+e^{-a(1-ANOX-c)}}\left(\frac{DOC}{DOC_0}\right), & DOC \geq 1 \times 10^{12}\ mol \end{cases} \quad (3)$$

here $a = 300$, $c = 0.35$ and $k = 1 \times 10^{14}$ mol yr^{-1} are scaling parameters for the sigmoid function, which define the anoxia level at which DOC oxidation begins and the rapidity of the transition. In practice, this function allows for geologically-rapid oxidation of DOC when ANOX < 0.7. The threshold here is chosen to be slightly below the model steady state so that the DOC reservoir is stable under the COPSE Ediacaran setup. DOC oxidation is terminated when the reservoir becomes smaller than 10^{12} moles, rather than zero, to prevent system instability. The rate of DOC oxidation is controlled by O_2 supply and never reaches the value

of k. This is shown in the SI for different values of c. We assume that DOC is oxidised directly by O_2, although oxidation via microbial sulfate reduction is also possible.

Sulfate input

An uplift and evaporite dissolution event is prescribed in the model using a simple step-forcing that follows previous work on evaporite dissolution[5]. The time-dependent forcing function for sulfate input is:

$$S_{input} = [0\ 1\ 10\ 16], [0\ 7\ 7\ 0] \quad (4)$$

where the first bracket is time in million years and the second bracket is the additional sulfate input in terms of the background weathering fluxes. For the model run in the manuscript, steady state 'background' and additional 'pulse' inputs of both pyrite and gypsum are considered:

$$gypw_{background} = k_{gypw} \cdot g_{runoff} \quad (5)$$

$$gypw_{pulse} = k_{gypw} \cdot g_{runoff} \cdot S_{input} \quad (6)$$

$$pyrw_{background} = k_{pyrw} \cdot g_{runoff} \quad (7)$$

$$pyrw_{pulse} = k_{pyrw} \cdot g_{runoff} \cdot S_{input} \quad (8)$$

here k_{gyp} and k_{pyr} are the present day weathering rates of gypsum and pyrite, and g_{runoff} is a climate-dependence representing the effect of global runoff on weathering fluxes, e.g. Berner (1994)[42]:

$$g_{runoff} = 1 + 0.087(T - T_0) \quad (9)$$

where T is global average surface temperature and T_0 is the present day value.

Sulfate burial

The COPSE model assumes that sulfate burial fluxes are linearly proportional to the total oceanic sulfate concentration, which means that concentration would have to rise to many times the present day level in order to bury large amounts of pyrite. We add an additional flux of pyrite burial ($mpsb_{additional}$) that is directly related to the pulsed weathering input of sulfate, so pyrite burial is more clearly related to the sulfate supply to high-productivity near-shore environments. A partitioning constant f_{py} is used to determine what fraction of the pulsed sulfate input is buried as pyrite. This is set at 0.8 in the plot shown in the ms. Additional sulfate that is not buried as pyrite is assumed to be buried as gypsum:

$$mpsb_{additional} = fpy \cdot (pyrw_{pulse} + gypw_{pulse}) \quad (10)$$

$$mgsb_{additional} = (1 - fpy) \cdot (pyrw_{pulse} + gypw_{pulse}) \quad (11)$$

Other model alterations

The following alterations are made to COPSE to make the model more applicable to the scenario being tested:

1. COPSE uses a sigmoid function to calculate the degree of ocean anoxia, ANOX. A modified version of the function was previously presented[30], based on the anoxia response of 3D ocean models. Whilst the functions are similar and the choice makes little difference in the Phanerozoic version of COPSE, the Watson et al. version of the function has a more gradual transition to anoxia and allows the model to more easily assume an 'Ediacaran-like' steady state under minimal alteration of other parameters and is therefore used here.
2. COPSE predicts low $\delta^{13}C$ values for the Ediacaran steady state (~-2‰). In order to clearly test the size of the evaporite-induced excursion, we set the overall crustal carbonate reservoir $\delta^{13}C$ value to 2‰, which raises the $\delta^{13}C$ value of

carbon inputs and makes newly formed $\delta^{13}C_{carb}$ is ~0‰. This alteration merely shifts the baseline of $\delta^{13}C$.

3. We take crustal values of $\delta^{34}S_{pyrite}$ = 0‰ and $\delta^{34}S_{gypsum}$ = 30‰ to reproduce Ediacaran pre-excursion baseline values[16], and assume that the pulse of evaporite weathering has $\delta^{34}S_{gypsum}$ = 15‰.
4. COPSE has a relatively high rate of gypsum weathering and burial at present day, we alter the present day reference rate of gypsum weathering to 1×10^{12}mol S yr^{-1}, to better represent the background rate used in ref 5, for which our evaporite dissolution scenario is based.

3. Additional model experiments

See supplementary information 1 for additional model runs where we assume no climate dependence for sulfur weathering fluxes, and consider the role of pyrite versus gypsum weathering, and test uncertainty in the DOC oxidation function.

4. Full model description

See supplementary information 2 for full modified COPSE model equations and description. MATLAB code for COPSE is freely available at https://github.com/sjdaines/COPSE/releases

References

1. Lenton, T. M., Boyle, R. A., Poulton, S. W., Shields-Zhou, G. A. & Butterfield, N. J. Co-evolution of eukaryotes and ocean oxygenation in the Neoproterozoic era. Nat. Geosci. **7**, (2014).
2. Chen, X. et al. Rise to modern levels of ocean oxygenation coincided with the Cambrian radiation of animals. Nat. Commun. **6**, 1–7 (2015).

399 3. Rothman, D. H., Hayes, J. M. & Summons, R. E. Dynamics of the Neoproterozoic
400 carbon cycle. Proc. Natl. Acad. Sci. USA **100**, 8124–8129 (2003).

401 4. Knoll, A. H., Hayes, J. M., Kaufman, a J., Swett, K. & Lambert, I. B. Secular
402 variation in carbon isotope ratios from Upper Proterozoic successions of Svalbard and
403 East Greenland. Nature **321**, 832–838 (1986).

404 5. Burns, S. J. & Matter, A. Carbon isotopic record of the latest Proterozoic from Oman.
405 Eclogae Geol. Helv. **86**, 595–607 (1993).

406 6. Kaufman, A. J., Knoll, A. H. & Narbonne, G. M. Isotopes, ice ages, and terminal
407 Proterozoic earth history. Proc. Natl. Acad. Sci. U. S. A. **94**, 6600–6605 (1997).

408 7. Calver, C. R. Isotope stratigraphy of the Ediacarian (Neoproterozoic III) of the
409 Adelaide Rift Complex, Australia, and the overprint of water column stratification.
410 Precambrian Res. **100**, 121–150 (2000).

411 8. Melezhik, V., Fallick, A. E. & Pokrovsky, B. G. Enigmatic nature of thick sedimentary
412 carbonates depleted in 13C beyond the canonical mantle value: The challenges to our
413 understanding of the terrestrial carbon cycle. Precambrian Res. **137**, 131–165 (2005).

414 9. Grotzinger, J. P., Fike, D. a. & Fischer, W. W. Enigmatic origin of the largest-known
415 carbon isotope excursion in Earth's history. Nat. Geosci. **4**, 285–292 (2011).

416 10. Schrag, D. P., Higgins, J. A., Macdonald, F. A. & Johnston, D. T. Authigenic
417 carbonate and the history of the global carbon cycle. Science (80-.). **339**, 540–3
418 (2013).

419 11. Li, Z. X. et al. Assembly, configuration, and break-up history of Rodinia: A synthesis.
420 Precambrian Res. (2008). doi:10.1016/j.precamres.2007.04.021

421 12. Krissansen-Totton, J., Buick, R. & Catling, D. C. A statistical analysis of the carbon

isotope record from the Archean to Phanerozoic and implications for the rise of oxygen. Am. J. Sci. **315**, 275–316 (2015).

13. Fairchild, I. J. et al. Tonian-Cryogenian boundary sections of Argyll, Scotland. Precambrian Res. 1–28 (2017). doi:10.1016/j.precamres.2017.09.020

14. McKirdy, D. M. et al. A chemostratigraphic overview of the late Cryogenian interglacial sequence in the Adelaide Fold-Thrust Belt, South Australia. Precambrian Research **106**, 149–186 (2001).

15. Rose, C. V. et al. Constraints on the origin and relative timing of the Trezona ?? 13C anomaly below the end-Cryogenian glaciation. Earth Planet. Sci. Lett. **319**–**320**, 241–250 (2012).

16. Fike, D. A, Grotzinger, J. P., Pratt, L. M. & Summons, R. E. Oxidation of the Ediacaran ocean. Nature **444**, 744–7 (2006).

17. Lu, M. et al. The DOUNCE event at the top of the Ediacaran Doushantuo Formation, South China: Broad stratigraphic occurrence and non-diagenetic origin. Precambrian Res. **225**, (2013).

18. Condon, D. et al. U-Pb ages from the Neoproterozoic Doushantuo Formation, China. Science **308**, 95–98 (2005).

19. Gong, Z., Kodama, K. P. & Li, Y. X. Rock magnetic cyclostratigraphy of the Doushantuo Formation, South China and its implications for the duration of the Shuram carbon isotope excursion. Precambrian Res. **289**, 62–74 (2017).

20. Bristow, T. F. & Kennedy, M. J. Carbon isotope excursions and the oxidant budget of the Ediacaran atmosphere and ocean. Geology **36**, 863–866 (2008).

21. Bjerrum, C. J. & Canfield, D. E. Towards a quantitative understanding of the late

445 Neoproterozoic carbon cycle. Proc. Natl. Acad. Sci. U. S. A. **108**, 5542–5547 (2011).

446 22. Derry, L. A. A burial diagenesis origin for the Ediacaran Shuram-Wonoka carbon
447 isotope anomaly. Earth Planet. Sci. Lett. **294**, 152–162 (2010).

448 23. Li, C. et al. Uncovering the spatial heterogeneity of Ediacaran carbon cycling.
449 Geobiology **15**, 211–224 (2017).

450 24. Lee, C., Love, G. D., Fischer, W. W., Grotzinger, J. P. & Halverson, G. P. Marine
451 organic matter cycling during the Ediacaran Shuram excursion. Geology **43**, 1103–
452 1106 (2015).

453 25. Garrels, R. M. & Lerman, A. Coupling of the sedimentary sulfur and carbon cycles -
454 an improved model. Am. J. Sci. 989–1007 (1984).

455 26. Burke, A. et al. Sulfur isotopes in rivers: Insights into global weathering budgets,
456 pyrite oxidation, and the modern sulfur cycle. Earth Planet. Sci. Lett. (2018).
457 doi:10.1016/j.epsl.2018.05.022

458 27. Wortmann, U. G. & Paytan, A. Rapid variability of seawater chemistry over the past
459 130 million years. Science (80-.). **337**, 334–336 (2012).

460 28. Guilbaud, R., Poulton, S. W., Butterfield, N. J., Zhu, M. & Shields-Zhou, G. A. A
461 global transition to ferruginous conditions in the early Neoproterozoic oceans. Nat.
462 Geosci. **8**, (2015).

463 29. Lenton, T. M., Daines, S. J. & Mills, B. J. W. COPSE reloaded: An improved model of
464 biogeochemical cycling over Phanerozoic time. Earth-Science Rev. **178**, 1–28 (2017).

465 30. Daines, S. J., Mills, B. J. W. & Lenton, T. M. Atmospheric oxygen regulation at low
466 Proterozoic levels by incomplete oxidative weathering of sedimentary organic carbon.
467 Nat. Commun. **8**, (2017).

468 31. Canfield, D. E. & Farquhar, J. Animal evolution, bioturbation, and the sulfate
469 concentration of the oceans. Proc. Natl. Acad. Sci. U. S. A. **106**, 8123–8127 (2009).

470 32. Osburn, M. R., Owens, J., Bergmann, K. D., Lyons, T. W. & Grotzinger, J. P.
471 Dynamic changes in sulfate sulfur isotopes preceding the Ediacaran Shuram
472 Excursion. Geochim. Cosmochim. Acta **170**, 204–224 (2015).

473 33. Laakso, T. A. & Schrag, D. P. A small marine biosphere in the Proterozoic.
474 Geobiology (2019). doi:10.1111/gbi.12323

475 34. Kendall, B. et al. Uranium and molybdenum isotope evidence for an episode of
476 widespread ocean oxygenation during the late ediacaran period. Geochim. Cosmochim.
477 Acta **156**, 173–193 (2015).

478 35. Shi, W. et al. Sulfur isotope evidence for transient marine-shelf oxidation during the
479 Ediacaran Shuram Excursion. Geology **46**, 267–270 (2018).

480 36. Campbell, I. H. & Squire, R. J. The mountains that triggered the Late Neoproterozoic
481 increase in oxygen: The Second Great Oxidation Event. Geochim. Cosmochim. Acta
482 **74**, 4187–4206 (2010).

483 37. Prince, J. K. G., Rainbird, R. H. & Wing, B. A. Evaporite deposition in the mid-
484 Neoproterozoic as a driver for changes in seawater chemistry and the biogeochemical
485 cycle of sulfur. Geology (2019). doi:10.1130/g45464.1

486 38. Saltzman, M. R. & Thomas, E. Chapter 11 - Carbon Isotope Stratigraphy. in The
487 Geologic Time Scale 207–232 (2012). doi:http://dx.doi.org/10.1016/B978-0-444-
488 59425-9.00011-1

489 39. Canfield, D. E., Poulton, S. W. & Narbonne, G. M. Late-Neoproterozoic Deep-Ocean
490 Oxygenation and the Rise of Animal Life. Science (80-.). **315**, 92–95 (2007).

40. Chen, X. et al. Rise to modern levels of ocean oxygenation coincided with the Cambrian radiation of animals. Nat. Commun. **6**, (2015).

41. Sahoo, S. K. et al. Oceanic oxygenation events in the anoxic Ediacaran ocean. Geobiology **14**, (2016).

42. Berner, R. A. GEOCARB II: a revised model of atmospheric CO2over Phanerozoic time. Am. J. Sci. (1994). doi:10.2475/ajs.294.1.56